



# Enhancing the low frequency vibration reduction performance of plates with embedded Acoustic Black Holes

Stephen C. CONLON<sup>1</sup>; John B. FAHNLIN<sup>1</sup>; Fabio SEMPERLOTTI<sup>2</sup>; Philip A. FEURTADO<sup>1</sup>

<sup>1</sup> Applied Research Laboratory, Pennsylvania State University, State College, PA, USA

<sup>2</sup> Aerospace and Mechanical Engineering, University of Notre Dame, Notre Dame, IN, USA

## ABSTRACT

Embedded Acoustic Black Holes (ABH) have been investigated as a passive treatment for noise and vibration control. The ABH effect is produced from a plate thickness power taper which results in a local asymptotic reduction of wave speed within the ABH. Theoretically the local wave speed approaches zero at the ABH center, causing the waves to take an infinite amount of time to reach the center, thus the waves are “trapped” in the black hole. This work focused on the low frequency performance of plates with periodic grids of ABHs for structural vibration and radiated sound reduction. Plates with embedded ABH grids were modeled with detailed Finite / Boundary Element models. The results show the ABHs reduce the narrow band vibration and radiated sound power by up to approximately 20 dB or more over that of the heavier uniform panel, at frequencies below the theoretical cut-on of the ABH as a broadband absorber. The low frequency performance of the ABH grids can be tailored based on the low frequency vibration characteristics of the ABH unit cell. Detailed results for several ABH plate configurations are presented giving insight into key ABH low frequency design performance characteristics.

Keywords: Damping, Noise reduction, Transmission loss, I-INCE Classification of Subjects Number(s): 38.5, 43.2.1, 47.3

## 1. INTRODUCTION

Embedded Acoustic Black Holes (ABH) have shown significant benefits as passive treatments for noise and vibration control (1-5). The ABH effect is produced from a plate thickness power taper which results in a local asymptotic reduction of wave speed within the ABH feature. Theoretically the local wave speed approaches zero at the ABH center, causing the waves to take an infinite amount of time to reach the center, thus the waves are “trapped” in the black hole. In practice the wave speeds never vanish due to a finite taper termination thickness. The ABH features act to focus the vibrational energy of the plate where it can then be effectively damped within the ABH using an added high loss damping layer, or extracted from the system via an energy harvesting elements (6). This work focused on the low frequency performance of plates with periodic grids of ABHs for structural vibration and radiated sound reduction. ABH theory addresses vibration absorption characteristics at frequencies where the plate bending wavelengths are smaller than the ABH characteristic dimension. For many applications of interest, such as vehicle systems, structural constraints may limit the size of an embedded ABH feature, yet also demand low frequency performance to meet vibration and noise reduction goals. These competing requirements could limit the applicability of embedded ABHs as potential design solutions, unless methods for quantifying and tailoring ABH low frequency performance are developed. This work focused on plates with embedded ABH grids modeled using detailed Finite Element (FE) models, with air loading modeled with coupled Boundary Element (BE) models, to examine vibration and radiated sound power performances due to specified force excitations. Total modal loss factors and modal densities can also be computed in order to examine the plate structure’s low frequency performance. The overall goal of this investigation was to develop detailed results for prototypical periodic grid ABH plate configurations examining the role of the ABH

---

<sup>1</sup> scc135@arl.psu.edu

cell, its low frequency dynamics, and the role of ABH cell / grid low frequency modal density in noise and vibration control.

## 2. THEORY

The concept of a Black Hole was first proposed by Pierre Simon Laplace in 1795. Using Newton's theory of gravity, Laplace predicted that if an object was compressed to a small enough radius, the escape velocity of the object would be faster than the speed of light. If the path of light is far from a black hole, there is no effect. However, as the path approaches the black hole, there is at first a small deflection in the path, with increasing path deflection in closer range, and ultimately with the path entering the event horizon the deflected path is so curved that the light cannot escape. The black hole is a singularity point in space, and as such possesses two key characteristics, zero volume and infinite mass.

Mironov (1) observed a similar effect in structures, for structures this was later coined the "Acoustic Black Hole" effect by Krylov (2). Mironov calculated the wave propagation in plates observing there were theoretically no reflections of waves for a plate with a thickness which decreases smoothly to zero over a finite interval. The wave speed asymptotically decreases so the wave takes an infinite time to reach the end of the taper, thus there is no reflected component and the tapered feature acts like a "Black Hole." Recently many other authors have examined fundamental one and two dimensional ABH concepts both theoretically and experimentally.

Assuming rotary inertia and shear effects are small, the thin plate bending wave speed can be written as

$$c_b = \left[ 2\pi f \left( \frac{h}{2\sqrt{3}} \right) \sqrt{\frac{E}{\rho(1-\nu^2)}} \right]^{\frac{1}{2}} \quad (1)$$

where  $f$  is the frequency,  $h$  is the plate thickness,  $E$  is the modulus of elasticity,  $\rho$  is the density, and  $\nu$  is the Poisson's ratio. For a plate of length  $L$ , with uniform thickness from 0 to  $L/2$  and a power taper from  $L/2$  to  $L$ , the wave speed in the tapered region becomes

$$c_{b-taper} = \text{constant } f^{\frac{1}{2}} L-x^{\frac{m}{2}} \quad (2)$$

where  $h(x) = h_f$ ,  $0 \leq x \leq L/2$  the full uniform plate thickness, and  $h(x) = \varepsilon L-x^m$ ,  $L/2 < x \leq L$  the tapered plate thickness. The resulting wave speed asymptotically approaches zero as the taper thickness approaches zero at the tip. As Mironov (1) showed, however, the tip of the ABH is a singularity condition where the wave speed vanishes, but in addition the singularity condition dictates that the velocity amplitude of the vibration becomes infinite

## 3. MODELS AND ANALYSES

Plates with embedded ABH grids were modeled with detailed Finite Element (FE) models, with the active and reactive air loading modeled with coupled Boundary Element (BE) models. Uniform plates were also modeled to serve as relative baselines to the ABH designs. The ABH plate models incorporated a full  $5 \times 5$  (25-ABH) periodic grid, and a truncated (13-ABH) grid of ABH elements (Fig. 1). The uniform and ABH panels were nominally 6.8 mm thick aluminum. The mesh resolutions were refined in order to fully resolve the vibration and acoustic fields at the highest frequencies of interest. Figure 2 shows an example of the FE mesh within the ABH. The plate and damping layers were modeled using quadratic brick elements. The acoustic mesh used in the boundary element analyses were the same as the structural mesh (for the ABH panel just the uniform side of the plates were fluid loaded). The ABH features had an outer diameter of approximately 10 cm, a taper of  $m=2.2$ , a 2 mm (free) damping layer (material damping loss factor of 0.10) on the surface of the ABH taper region. The ABH panels had an outer diameter to center hole diameter ratio of  $OD/ID=10$ . The rows and columns of ABH cells were spaced approximately 4 cm from each other. The uniform panel had added damping circular patches in the same locations as the  $5 \times 5$  ABH plate to capture the "equivalent" amount of added damping layer.

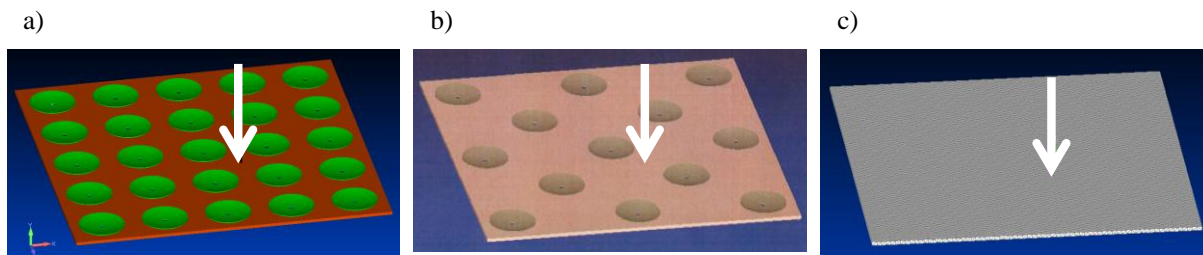


Figure 1: ABH and uniform panels with point force drives. a) Five by five grid 25-ABH panel, b) 13-ABH panel and c) uniform panel.

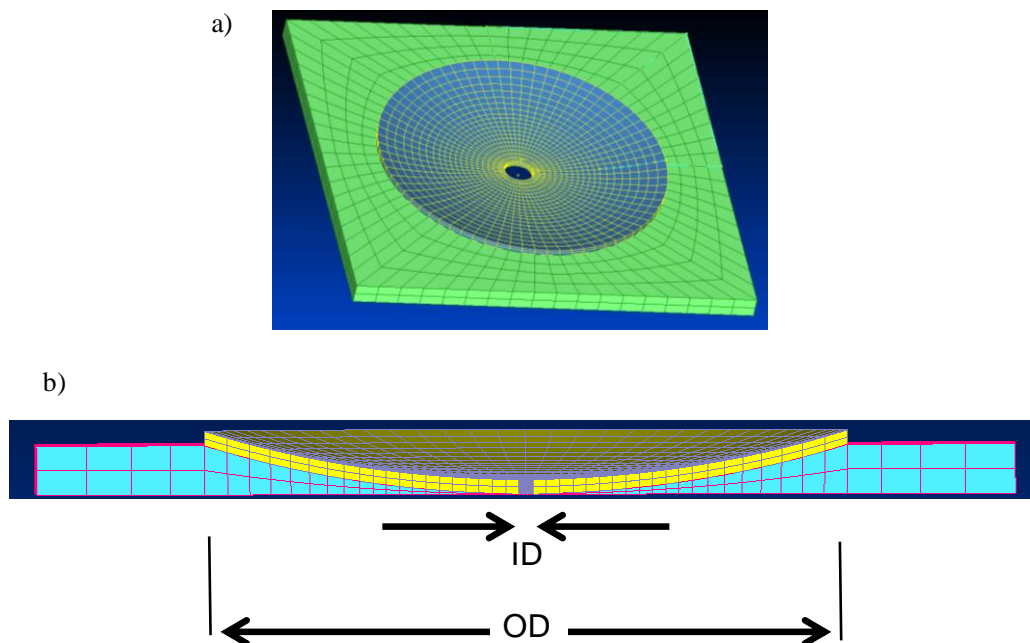


Figure 2: ABH cell, aspect ratio, and finite element mesh. a) ABH unit cell outer and inner diameters b) ABH unit cell cross-section with damping layer shown in yellow.

Forced response analyses were performed to quantify the designs radiated sound power characteristics. Total modal loss factors were also computed both with and without structural-acoustic radiation losses in order to examine the roles mechanical damping vs acoustic radiation damping play in the total effective damping of the plate structures. The commercial finite element code NX/NASTRAN (7) was used to analyze the FE models which characterize both the uniform baseline and the ABH panels' vibration characteristics. The acoustic / radiated sound power analyses were performed using the boundary element code POWER (8). The surrounding acoustic medium was air so the resonance frequencies for the panels did not shift significantly due to fluid coupling, but acoustic radiation damping did change the overall damping levels. The coupled FE/BE computations were performed using a modal frequency response formulation. The *in vacuo* structural modes were used as basis functions, with an extra term added into the equations of motion to represent the forces input back into the structure due to the acoustic pressure field. Air loading, both reactive and resistive, was considered on one side of the panels (for the ABH panel to side opposite the ABH features), with free mechanical boundary conditions and a baffled acoustical boundary (panels radiating into half space). A unit force point drive was applied and the surface averaged acceleration and total radiated sound power computed. The panel total masses were: uniform= 9.5 kg and 25-ABH= 7.6 kg. The uniform plate critical frequency was estimated at approximately 1900 Hz.

#### 4. RESULTS

Figure 3 shows the radiated sound power and surface averaged acceleration results for the ABH and uniform panels. The ABH plate shows up to 20 dB or more vibration and sound power reductions above 2,500 Hz due to the ABH features. Note the ABH panel is 20% lighter than the uniform panel. Below 2,500 Hz, the ABH panel shows lower sound power for some frequencies and higher sound power at other frequencies, but with similar amplitude trends.

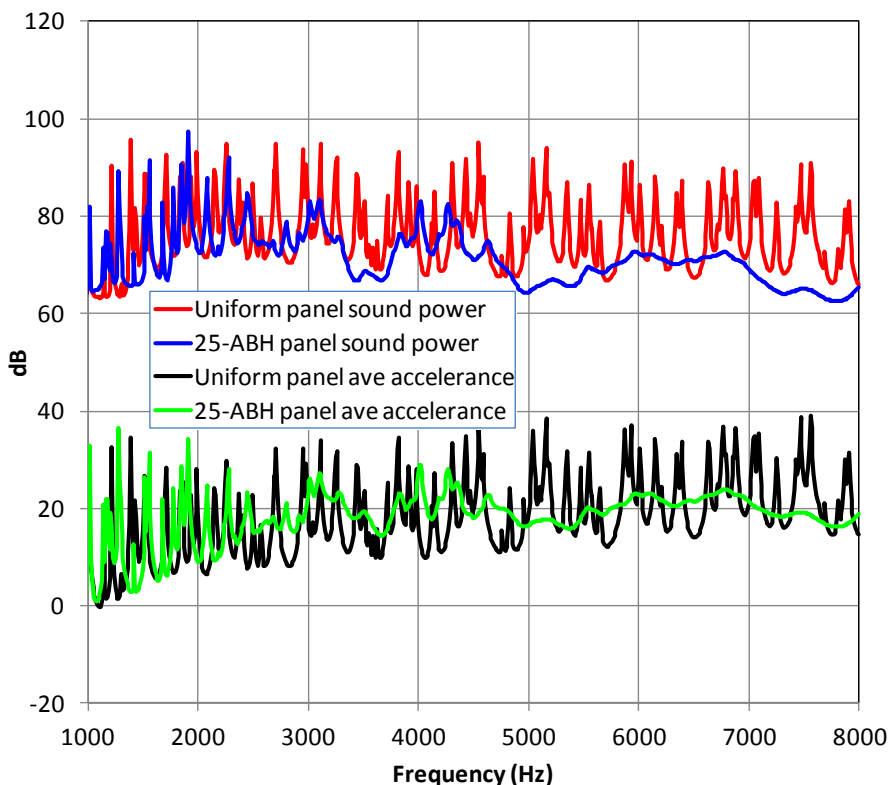


Figure 3: ABH and uniform panel responses for harmonic point force drives. Total radiated sound power output, dB re  $1 \times 10^{-12} \text{ W/N}^2$  (top), and surface averaged acceleration, dB re  $1 \text{ m/s}^2/\text{N}$  (bottom).

Above approximately 6,500 Hz, the frequency where the plate bending wavelength equals the ABH outer diameter, the ABHs are expected to act as broadband absorbers. Figure 3 showed substantial vibration reduction well below 6,500 Hz in the typical low / mid frequency range often of interest for vehicle systems. A closer examination of the ABH panel performance is examined by computing the modal loss factors up to 8,000 Hz. Figures 4 and 5 modal loss factor results for the ABH panel vs uniform panel. Figure 4 includes the resistive air loading, clearly showing the effects of acoustic radiation damping near and above the plate critical frequency of 1900 Hz. Figure 5 show the loss factor results with the air resistive loading removed. The ABHs increase the mechanical damping of the panel by approximately a factor of thirty five for much of the frequency band from 2,500 Hz to 8,000 Hz. The peaks in ABH modal loss factors around 2,600 Hz, 3,500 Hz and 5,000 Hz are due to low order modes within the ABH cells. The ABH panel low/mid frequency performance is strongly dependent on these low order ABH local modes. The 2,600 Hz / 3,500 Hz / 5,000 Hz clusters of increased loss factor modes are predominantly  $n=0$  /  $n=1$  /  $n=2$  local ABH cell modes, where “n” refers to the number of waves around the circumference of the ABH. The clustering of modes around the loss factors peak values result from different phasing in the  $5 \times 5$  ABH grid of the individual ABH cells. To assess the sensitivity of the ABH performance to the modal density of the low frequency ABH cells, a second truncated grid of 13 ABH cells (Fig 1) was assessed.

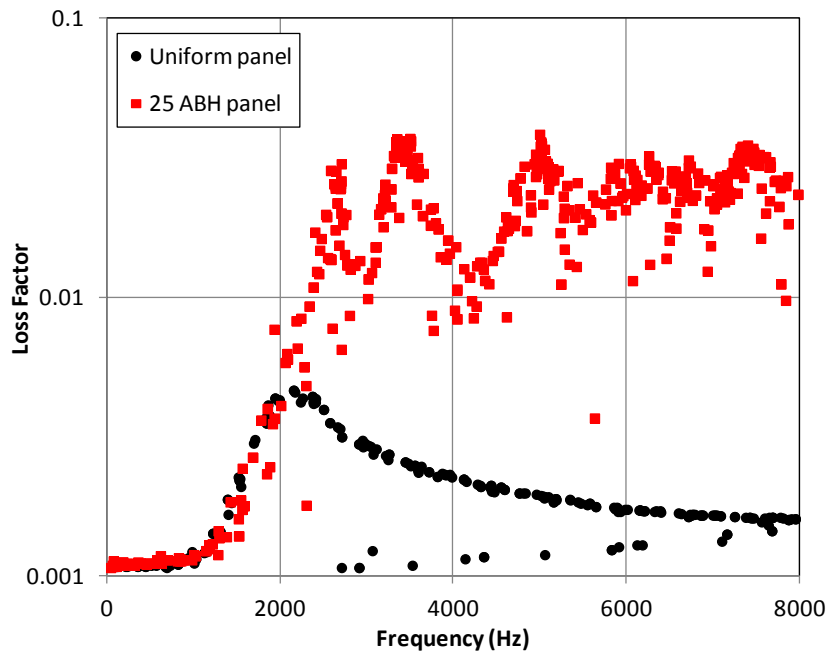


Figure 4: Modal loss factors including acoustic radiation damping for ABH panel vs uniform panel. The uniform panel critical frequency is approximately 1,900 Hz.

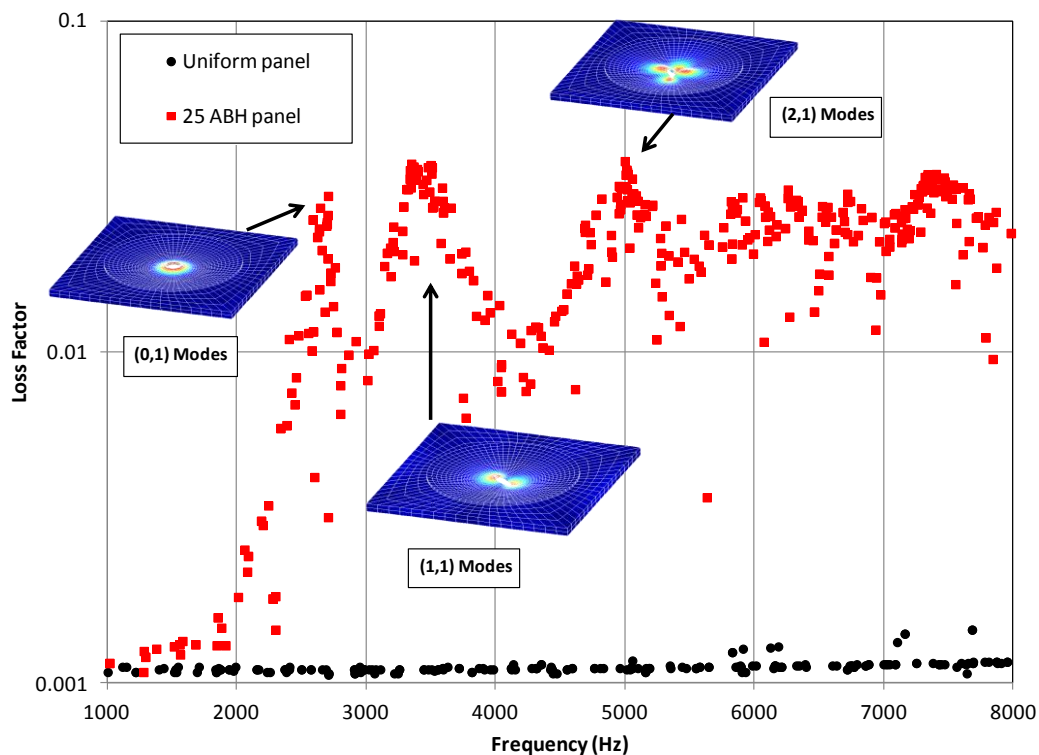


Figure 5: Modal loss factors without acoustic radiation damping for ABH panel vs uniform panel. The 2,600 Hz / 3,500 Hz / 5,000 Hz clusters of increased loss factor modes are predominantly  $n=0$  /  $n=1$  /  $n=2$  local ABH cell modes.

The modal loss factors for the two ABH panels, 25 and 13 ABH grids, are compared to the baseline uniform panel in Figure 6 (acoustic radiation damping removed). Similar  $n=0$  and  $n=1$  ABH cell modes appear for the 13- ABH panel, but as might be expected there are fewer local modes due to the reduced grid. Note the ABH cell geometry could be tailored to optimize the frequencies of the low-frequency-damping peaks for a given application. Care needs to be taken, however, when designing the ABH cell to enhance low frequency performance, in order to maintain properties that adhere to the theoretical ABH smoothness requirements (1). Above approximately 5,500 Hz the modal loss factor trend is more uniform as the ABHs start to perform as broadband absorbers and their performance becomes less dependent on discrete internal cell modes. Figure 7 compares the cumulative mode counts for the three panels, clearly showing the growth due to the local ABH cell modes above approximately 2,500 Hz. Theoretically a thin uniform plate would have a constant modal density, which the uniform panel follows showing a nearly constant slope cumulative mode count in Figure 7. The increase in cum mode count of the 13-ABH panel over the uniform panel up to 2,800 Hz is approximately 20 modes. This is the same mode count increase for the 25-ABH panel over that of the 13-ABH panel, as might be expected due to the doubling of ABH cells.

Figure 8 compares the radiated sound power for the 25-/13- ABH designs, which can be compared to the baseline uniform panel in Figure 3. The effects of enhanced modal damping, as were shown in Figure 6, as well as the differences in modal density contribute to the ABH sound power reductions. At the ABH cell mode clusters of 2,600 Hz / 3,500 Hz / 5,000 Hz there is the most sound power reduction by the ABH panels, with the 25-ABH panel showing about 3 dB more reduction than the 13-ABH panel (noise reduction scales linearly by cell count). At the side band frequencies around 2,600 Hz / 3,500 Hz / 5,000 Hz there is still significant improvement over the uniform panel, but a mix of performance at a given frequency between the 25-/13- ABH panels. At high frequencies, above 6,500 Hz, the ABH panel's sound power results show substantial reductions over the uniform panel and are also less peaked over the band of frequencies assessed. In the high frequency limit the 25-ABH panel is expected to have an average of 3dB increase in sound power reduction over that of the 13-ABH panel.

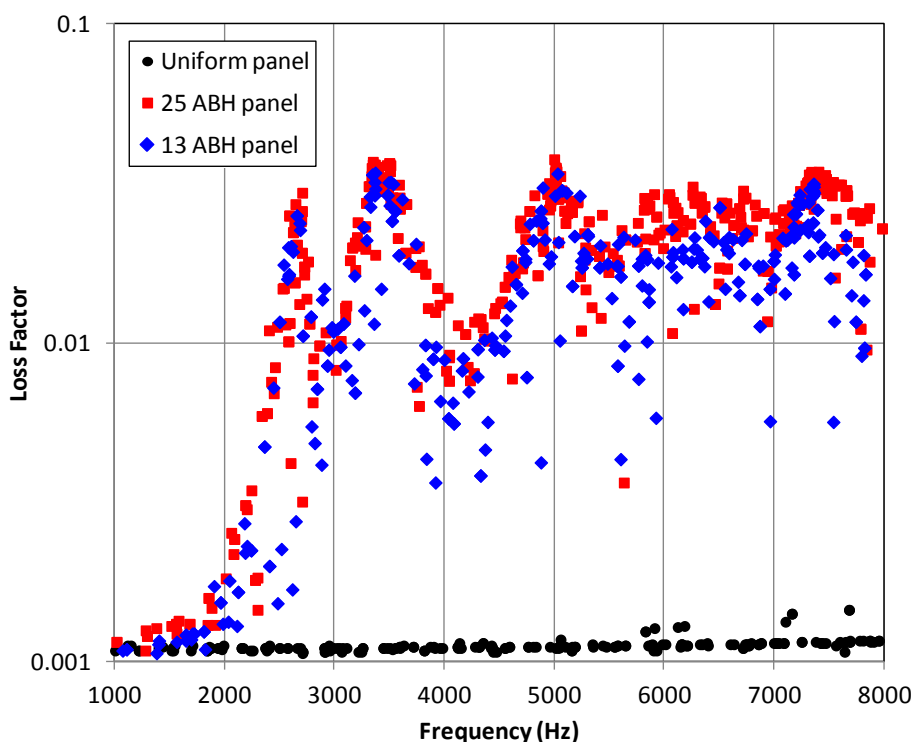


Figure 6: Modal loss factors without acoustic radiation damping for ABH panels (25-ABH and 13-ABH grids) vs uniform panel. The low order mode peak levels in LF are the same, but the 25-ABH panel has a higher number of local ABH cell modes.

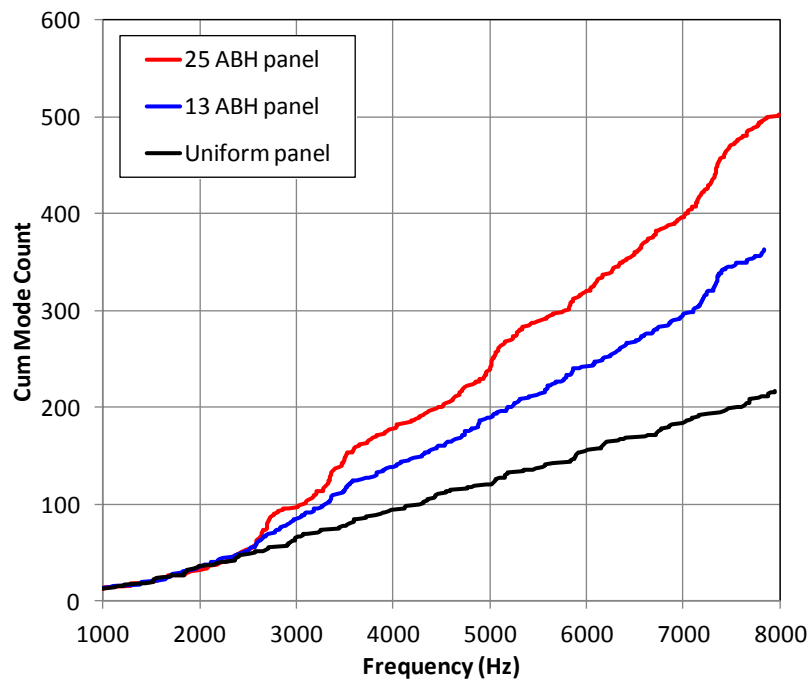


Figure 7: Mode count ABH and uniform panels. Increases in modal density due to the 25-ABH and 13-ABH grids are significant above approximately 2,500 Hz.

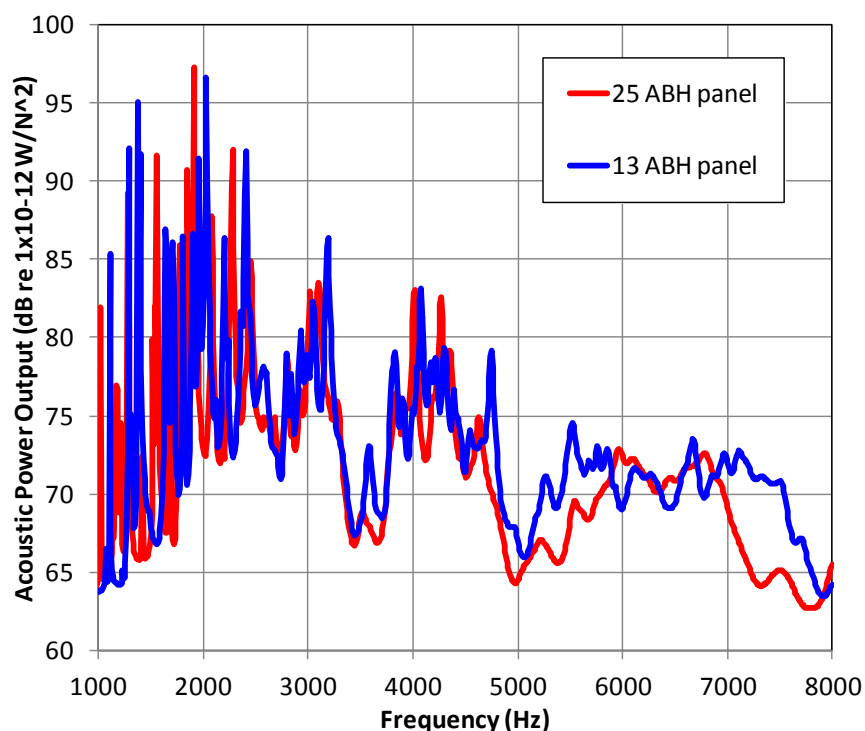


Figure 8: ABH panel total radiated sound power output (dB re  $1 \times 10^{-12} \text{ W/N}^2$ ). At the ABH cell mode clusters of 2,600 Hz / 3,500 Hz / 5,000 Hz there is the most sound power reduction by the ABH panels, with the 25-ABH panel showing about 3 dB more reduction than the 13-ABH panel.

## 5. CONCLUSIONS

The results showed the periodic grids of ABHs reduce the narrow band radiated sound power by up to 20+ dB over that of the heavier uniform panel. The role that ABH cell internal vibration

characteristics play in ABH low frequency performance was demonstrated. Methods for enhancing ABH low frequency performance were illustrated by assessing the size of the ABH periodic grid and the role that local ABH cell modes / modal density play in overall noise and vibration reduction. The results presented quantify the ABH potential for noise and vibration control and the potential for embedded ABH grids. Detailed results for several ABH grid configurations were compared and contrasted with uniform plate results, giving insight into several key ABH design performance parameters of interest to noise and vibration engineers. Future work will explore optimization of the ABH embedded grid for optimal noise / vibration reduction and weight minimization, examining ABH grid spacing, size, and unit cell parameters.

## REFERENCES

1. Mironov, M.A., Propagation of flexural waves in a plate whose thickness decreases smoothly to zero in a finite interval, *Sov. Phys. Acoust.* 34(3), (1988), pp. 318-319.
2. Krylov, V.V., Laminated plates of variable thickness as effective absorbers for flexural vibrations, *Proceedings of the 17th International Congress on Acoustics, Rome, Italy, 2-7 September 2001*, Ed. A. Alippi (2001), Vol. 1, pp. 270-271.
3. Krylov, V.V., Tilman, F.J.B.S., Acoustic 'black holes' for flexural waves as effective vibration dampers, *J. Sound and Vib.*, 274, (2004), pp 605-619.
4. Krylov, V.V., Winward, R.E.T.B., Experimental investigation of the acoustic black hole effect for flexural waves in tapered plates, *J. Sound and Vib.*, 300, (2007), pp 43-39.
5. Conlon, S.C., Semperlotti, F., and Fahline, J.B., Passive control of vibration and sound transmission for vehicle structures via embedded Acoustic Black Holes, *Noise-Con 2013, Denver Colorado, August 26-28 (2013)*.
6. Zhao, L., Conlon, S., and Semperlotti, F., Broadband Energy Harvesting using Acoustic Black Hole Structural Tailoring, *Smart Mater. Struct.*, 23 (2014).
7. NX/NASTRAN, Version 8.5 & Users Manual, Siemens PLM Software, Plano, TX.
8. Koopman, G.H., Fahline, J.B., *Designing Quiet Structures, A Sound Power Minimization Approach*, Academic Press (1997). The code POWER is written in FORTRAN and included with the text from Academic Press. POWER: A Numerical Implementation of the Lumped-Parameter Model for the Acoustic Radiation Problem. Written by: John B. Fahline Applied Science Building, The Pennsylvania State University, University Park, PA 16804.